Indian Journal of Chemical Technology
Vol. 29, November 2022, pp. 706-712
DOI: 10.56042/ijct.v29i6.67353

Preparation and characterization of hybrid nanofibrous polymer scaffolds for tissue engineering applications

Gurumoorthi Ramar[1], Sangeetha Ashokumar[1], Bhuvana K Periyasamy*[,1] & R Joseph Bensingh[2]

[1]Department of Petrochemical Technology, Central Institute of Petrochemical Engineering and Technology (CIPET), Chennai 600 032, India

[2]CIPET: School for Advanced Research in Polymers (SARP) - APDDRL, Bengaluru 562 149, India

E-mail: kpusha27@gmail.com

Received 19 August 2022; accepted 21 October 2022

This paper endeavours towards the scientific study of infusion of silver nanoparticles (Ag NPs) into biodegradable polymer scaffold for bone tissue engineering. Highly biocompatible Ag NPs have been synthesized using chitosan as stabilizing and reducing agent. The synthesized Ag NPs have been uniformly suspended in polyvinyl alcohol (PVA) and sodium alginate (SA) solution and nanofibrous mat like scaffolds have been fabricated using electrospinning process. The proposed process of infusing Ag NPs in PVA/SA medium resulted in nanofibers of smaller diameter and reduced pore size resulted in high surface area which is due to electrostatic charge interaction of Ag NPs during electrospinning. Thus, the improved surface area has facilitated better growth of extracellular matrix (ECM) compared to traditional coating method. The effect of coating nanoparticles on prepared polymeric scaffolds proves less than infusion of nanoparticles prior to electrospinning.

Keywords: Bone tissue engineering, Chitosan, Electrospinning, Silver, Sodium alginate

Tissue engineering (TE) is to develop cell and construct the living system technologies to restore the structures and functions of damaged or diseased tissues/organs. Biomaterials play a significant role in TE by serving as matrices for cellular in growth, cell proliferation, and formation of new tissue in three-dimensions. Research emphasize towards precise control of scaffold materials and its structure to improve the complexity and hence the quality of tissue formation. There is numerous work on development of nano-fibrous structures to mimic the extracellular matrix (ECM) or prepare scaffolds that act as an artificial ECM suitable for TE. The ultimate aim of TE is that these scaffolds are made to mimic collagen, a natural ECM component of nearly every tissue such as bone, skin, tendon, ligament, and so forth. Among these a huge research is dedicated towards bone TE. Human bone is a complicated system made up of hard and soft tissues and act as a structural and support of the human body. Bone is a combination of organic and inorganic components. Osteomyelitis causes bone destruction and sequestrum formation by bacterial infection for children. It depends on different factors like severity, types, virulence pathogens, and the physiological host[1]. This research involves regeneration or repairing the bone using implantation of isolated cells, delivering tissue-inducing substance (growth factor), and placing cells on or within different matrices. But nowadays, the damaged bone is treated using scaffolds like bio mimicking artificial and natural implants used for bone TE. The scaffold that mimics structural and functional properties of the ECM of bone is used for tissue repairing and remodeling. Bone scaffold material should be biocompatible and biodegradable with host tissues; non-toxic and non-immunogenic. Additionally, its mechanism and pore size must be suitable for bone and osteoconductivity in bone TE[2].

In bone tissue engineering, a lot of techniques are developed for fabricating three-dimensional scaffold, such as electrospinning, phase separation, freeze-drying, 3D printing, organ printing, self-assembly and regenerative medicine[3]. In these methods, the scaffold can mimic the architecture of the native ECM at the nano level (nanofibers, nanoporous, etc.) that provides space for the regeneration of new tissue[4]. Out of these techniques, electrospinning is a well-recognized method, and it permits the fabrication of scaffolds with similar morphology and mechanical behaviour as that of a native ECM[5]. The fabricated scaffold is highly used in treating damaged tissue, such as blood vessels, muscle, ligaments, skin, nerves, tendons, cartilage, and bones. Compared to a flat surface materials; nanofibers have a high surface area and

tiny pores, with the help of directional fiber alignment and more adhesive sites that spread quickly and migrate into specific directions[6]. The mechanical properties of nanofibers play a significant role in the bone TE. Hence, polymeric compositions have to be chosen in combination with inorganic materials[7].

Generally, natural polymers used in the electrospun are collagen, chitosan, silk fibrin, etc. and synthetic polymers used are polyethylene glycol (PEG), polyvinyl chloride (PVC), polyvinyl alcohol (PVA), etc[8]. The properties of natural polymer cannot be altered easily, hence research is focused towards synthesizing and using synthetic polymers. Among the synthetic polymers, PVA provides mechanical stability, slow degradation kinetics and flexibility even superior than natural polymers[9]. Moreover, the hydrophilic nature of PVA enables addition of cross linkers for better bone TE applications. Sodium alginate (SA) acts as a powerful cross-linker along with PVA that facilitates better biocompatibility, biodegradability[10]. However, as a polymer blend PVA/SA composition suffer from poor physical strength. Hence, addition of nanoparticle is preferred to improve the strength[11,12]. Silver nanoparticles (Ag NPs) have been reported to possess excellent antibacterial, anticancer activity properties and few studies reported that Ag NPs induce osteoblast bone formation[13]. Additionally, it is to be noted that $AgNP_S$ capped by chitosan will be efficient compared to Ag NPs decorated with other polymer. Because chitosan is derived from the deacetylation of chitin, which is a linear polysaccharide consisting of beta-1,4 linked N-acetylglucosamine units hence capable of better cell adherence and proliferation[14]. Therefore, chitosan is a promising choice for bone TE which is used as the reducing and stabilizing agent in silver preparation[15]. Thus, this work involves in addition of chitosan decorated Ag NPs into PVA/SA nanofibers in two methods (spray coating and direct infusion). Among these two methods, infusion of Ag NPs in polymeric solution to fabricate PVA/SA/Ag NPs nanofibres has not been reported for bone TEas far as our knowledge is concern[16]. Henceforth this article elaborates the effectiveness of infusing Ag NPs rather than traditional coating of nanoparticles on nanofiber mat[17].

Experimental Section

Preparation of chitosan mediated silver nanoparticles

Ag NPs were prepared by reducing silver nitrate ($AgNO_3$) using Chitosan supernant solution. The experimental procedure is as reported elsewhere[18]. It is stated that nanoparticles prepared using biopolymers were found to possess better antibacterial properties and improved biocompatibility than common chemical synthesis route.

Preparation of polymeric solutions

Three different polymeric solutions were prepared using water as a solvent in the following compositions: 100% PVA solution, 90:10 PVA/SA polymeric blend and 90:8:2 PVA/SA/Ag NPs polymer nanocomposite solution. Initially, 10wt% of PVA solution was prepared by dissolving an appropriate amount of PVA at 90°C hot distilled water which formed the pure PVA solution. For the preparation of PVA/SA blends 1 part of the sodium alginate (SA) (1.8 g) solution was added with 9 parts of pure PVA (18 g) solution upon stirring at 90°C for 2 h. To prepare PVA/SA/Ag NPs nanofibrous scaffolds, 20 mg of Ag NPs was ultrasonicated for 30 min in 5 mL of ethanol and mixed in the PVA/SA blend solution to acquire the polymer nanocomposite solution.

Preparation of polymeric nanofibers

Nanofibrous scaffolds were prepared using each of the above-mentioned polymer solutions through a free liquid surface electrospinning machine (ESPIN-nano). The solutions were loaded in a 2.5 mL plastic syringe with a 24G needle. Nanofibers were obtained by electrospinning the loaded solution for 5 h with a feed rate of 0.5 mL/h and the tip to collector distance ranging 15cm and applied voltage of 23 kV. The resultant fibers produced were collected by the cathode collector rotating drum covered with aluminium foil. The resultant nanofibers of different compositions were obtained after drying in room temperature for 12 h. The novelty of the work lies in the fact of blending PVA/SA/Ag NP in a single polymer solution by infusing Ag NPs for scaffold preparation. To examine the effect of infusion of Ag NPs in the polymer nanocomposite fibers, the traditional method of coating Ag NPs on PVA/SA was adopted. PVA/SA/Ag coated scaffolds were prepared by spray coating 20 mg of Ag NPs dispersed in 5 mL of ethanol on PVA/SA nanofibers at 40-50°C and drying in room temperature for 15 h for solvent removal. Later all these prepared scaffolds were transferred into desiccator until further analysis.

Physico-chemical characterization

Fourier transformed infrared (FTIR) spectroscopy was taken under ATR condition using a Nicolet

iS5-6700 model with the wavenumber ranging from 4000cm^{-1} to 400cm^{-1}. X-ray diffractograms were obtained using Rigaku Mini Flex XRD model with monochromatic copper radiation (Cuk$_\alpha$) of wavelength λ=1.54Å. SEM micrographs were acquired through field emission scanning electron microscopy (FESEM) –FEI quanta 200 model SEM. The absorbance spectra were recorded using HITACHI U-2900 spectrophotometer in the wavelength range of 190–800 nm in ambient conditions. *Invitro* studies were carried out by immersing of 1 cm × 2 cm scaffold in the simulated body fluid (SBF) solution. The surface changes and growth of extra cellular matrix in Ag embedded and Ag coated PVA/SA scaffolds before and after immersion in the SBF solution were obtained using scanning electron microscopy (SEM)-ZEISS MA15.

Results and Discussion

Characterization of chitosan-mediated Ag NPs

The structural characterization of synthesized Ag NPs was examined through FTIR and XRD analysis. Figure 1 illustrates the FTIR spectra of chitosan and Ag NPs. In the chitosan spectrum, the broadband at 3323 cm^{-1} is assigned for O-H stretching vibration indicating the existence of the hydroxyl group in the reducing agent and intramolecular hydrogen bond. The presence of residual N-acetyl groups was confirmed through the peaks at 1659 cm^{-1} (C=O stretching) and 1360 cm^{-1} (C-N stretching) corresponding to Amide I and Amide III, respectively[19]. The peak at 1208 cm^{-1} signifies the N-H deformation of Amide II[20]. While the FTIR spectrum of Ag NPs, the band at 3320 cm^{-1} denotes the presence of hydroxyl groups. The peak of 1639 cm^{-1} in chitosan is shifted to 1584 cm^{-1} due to the wagging of the NH_2 bond and the strong peak 1468 cm^{-1} is due to CH bending vibrations of the alkyl groups. The peak at 1360 cm^{-1} of chitosan shifted to the lower frequency of 1084 cm^{-1} in the case of the Ag NPs signifies that chitosan can perform a dual function of reduction and stabilization of silver nanoparticle[21]. The formation of Ag NPs is strongly confirmed through the presence of a peak at 520 cm^{-1} corresponds to Ag-O ionic bond[22]. The X-ray diffractogram of the Ag NPs are shown in Fig. 2. The diffraction peaks coincides with the JCPDS card No: 04-0783 indicating the formation of Ag NPs[23]. The obtained XRD pattern clearly illustrated that the silver ions have been reduced to AgO by the stabilization of chitosan.

The absorbance spectra shown in Fig. 3 revealed the formation of the Ag NPs. The UV-Vis

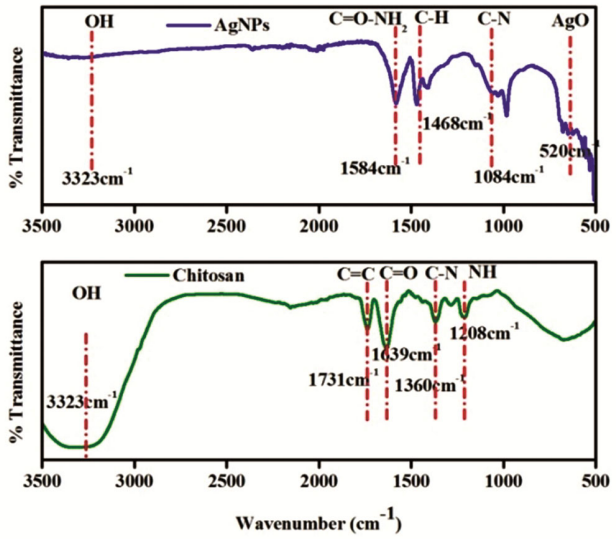

Fig. 1 — FTIR analysis chitosan mediated Ag NPs.

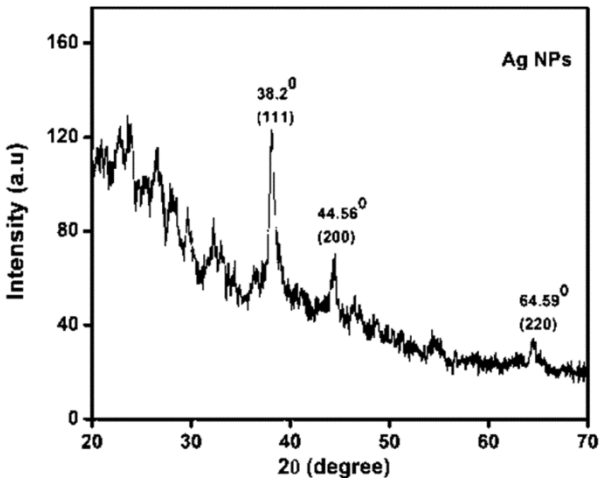

Fig. 2 — XRD diffractogram of chitosan mediated Ag NPs.

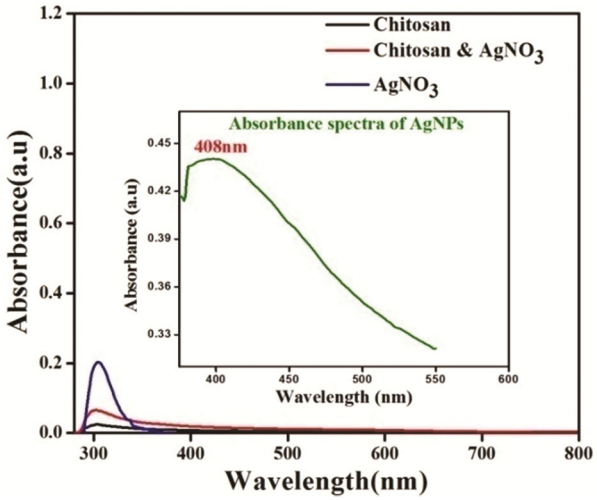

Fig. 3 — UV spectrum of chitosan mediated Ag NPs.

spectrum has no evidence of absorption in the range of 250-800 nm for the chitosan supernatant dissolved in distilled water[24]. The absorbance maxima at ~300 nm assigned to $AgNO_3$ has greatly reduced in intensity when mixed with Chitosan. The Chitosan - $AgNO_3$ solution in water displayed has an almost flat band due to the chelation of Ag^+ ions by the surface functional (hydroxyl and amine) groups of chitosan. Plasmon resonance derived from the silver nanoparticles is ~400nm displayed in the inset of Fig. 3. The blue shift in the absorbance maxima of Ag NPs in comparison to the bulk Ag (440nm) indicates the reduction in size of Ag and signifies the quantum confinement effect[25].

Figure 4 displays the SEM micrographs of synthesized Ag NPs. The particle are found to be in spherical shape with an average size 300 nm. Since the particles were confined, agglomeration of the particles are prevalently witnessed in the micrograph.

Characterization of nanofibers

Structural analysis and the presence of various constituents of PVA, SA, and Ag NPs in the nanofibers were confirmed through FTIR analysis. Comparative FTIR spectra of PVA, PVA/SA, PVA/SA/Ag NPs coated and PVA/SA/Ag NPs infused composite nanofibers were presented in Fig. 5 which signifies the changes in the spectrum with the addition of each component. In pure PVA Nanofibers, the broadband observed from 3100 to 3500 cm^{-1} was assigned to O-H stretching which was due to the strong intramolecular and intermolecular hydrogen bonds and the band at 2920 cm^{-1} was due to C-H alkyl stretching found in PVA[26]. FTIR spectrum of PVA/SA nanofibers displayed bands at 1576cm^{-1} and 1406 cm^{-1} which are assigned to asymmetric and symmetric stretching peaks of the carboxylate salt group (COO^-). Besides, the peak at 1407 cm^{-1} (OH)-C-(OH) bending, 1067 cm^{-1} (C-O stretching), 1024 cm^{-1} (C-O-C stretching), 847 cm^{-1} (C-OH stretching) confirmed the presence of SA[27,28]. The existence of Ag NPs on the nanocomposite fibers has been verified through the appearance of dip at 570 cm^{-1} attributed to the Ag-O bond[29]. The slight shift in the Ag-O peak from 520 to 570 cm^{-1} is owing to the interaction of the polymeric material with the NPs[22].

SEM micrographs of the polymer composite scaffolds at different compositions pure PVA, 90:10 (PVA/SA), and 90:8:2 (PVA/SA/ Ag NPsinfused) displays randomly oriented nanofibers. This randomness might support the fact of higher mechanical strength and biological properties. The fibrous structure of the scaffolds would result in a high surface area to volume ratio and interconnected porosity would be supportive for cell growth and proliferation. Figure 6 displays the micrographs of

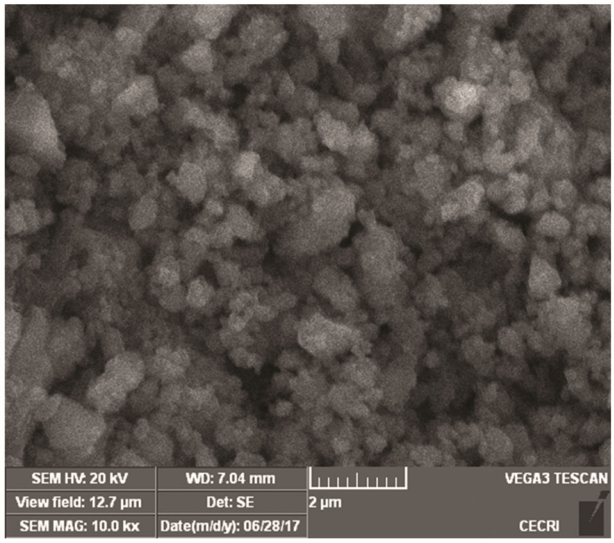

Fig. 4 — SEM micrographs of chitosan mediated Ag NPs.

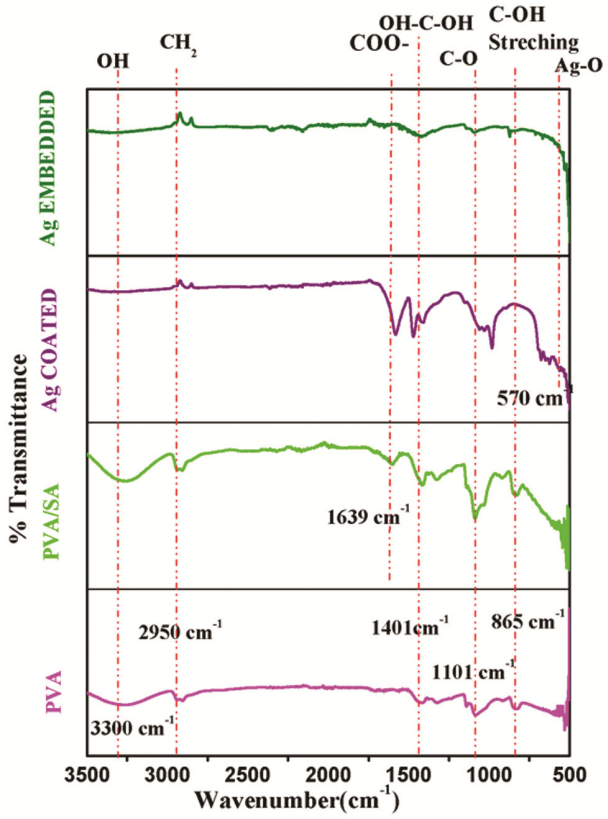

Fig. 5 — FTIR analysis of PVA, SA/PVA, Ag coated fiber (ethanol), Ag embedded fiber.

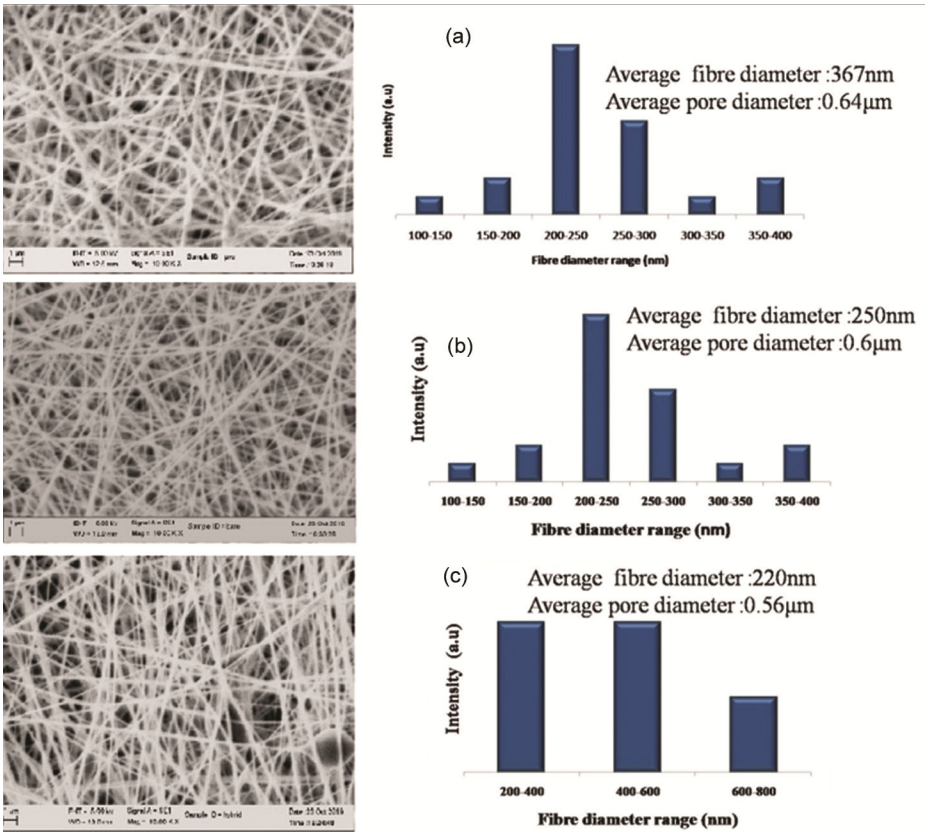

Fig. 6 — Morphology of electrospun fibers (a) PVA; (b) PVA/SA and (c) Ag embedded PVA/SA.

pure PVA nanofibers where the average diameter was 367 nm and the pore size was 0.64 µm. This micrograph shows that the pure PVA scaffolds have the largest fibers in diameter. In the case of the PVA/SA, nanofibers shows the uniform distribution and fibrous nature with an average fiber diameter of 250 nm and average pore size of 0.6 µm.The SEM images did not display any colour contrast in PVA/SA fibers which signifies the better miscibility of both the polymers[30]. The addition of Ag NPs in the blend polymeric solution has resulted in the extension of the fiber from the needle during electrospinning subsequently the hybrid fibers have a smaller diameter compare to other nanofibers. This effect is due to the charge interaction with the Ag NPs. Ag NPs are highly conductive in nature which brought about elongation of polymer fibers resulting in decrease in diameter of hybrid nanocomposite fibers. Thus, the average diameter of hybrid fibers is estimated to be 220 nm which is reduced 12 % compared to PVA/SA fiber and average pore size of 0.5 µm. The lesser fiber diameter with an increase in porosity paves the way for high surface area hence enhancing the possibility of better cell proliferation. Additionally, the Ag NPs present in the nanofibers have been reported to incorporate antibacterial properties. These hybrid nanocomposite scaffold are considered for *in vitro* analysis to examine the growth of ECM.

In vitro studies: Immersion of scaffolds in SBF solution

A comparative study on Ag coated and Ag infused PVA/SA nanofibers were performed. To examine the cell proliferation and growth ECM for TE application, the prepared scaffolds (2 cm × 2 cm) were immersed in the simulated body fluids (SBF) solution. SBF solution was prepared through Kokubo methods as reported earlier[31].

The prepared scaffolds were investigated through SEM to evaluate the surface changes before and after soaking in SBF solution. Figures 7 and 8 denote the surface characteristics of Ag infused and Ag coated polymer scaffolds. Both the scaffolds exhibited bioactivity. However, the Ag infused scaffolds displayed drastic changes from fibrous nature to condensed nature. The surface of the scaffolds was covered by a distinct layer of ECM. It can be derived from previous reports that the ECM formed can be

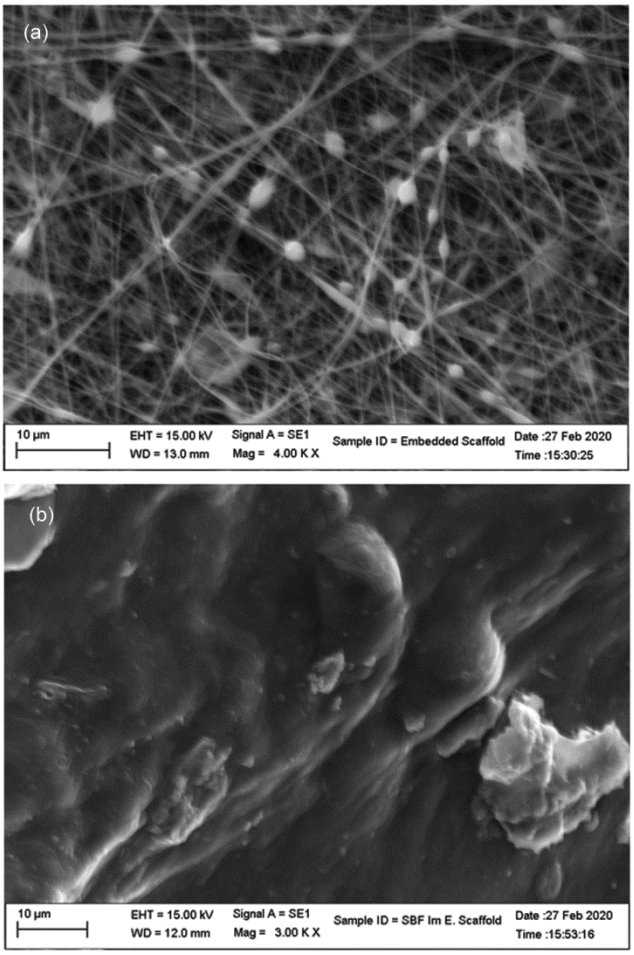

Fig. 7 — SEM micrograph of Ag embedded nanofiber (a) Before immersion and (b) After immersion in SBF solution.

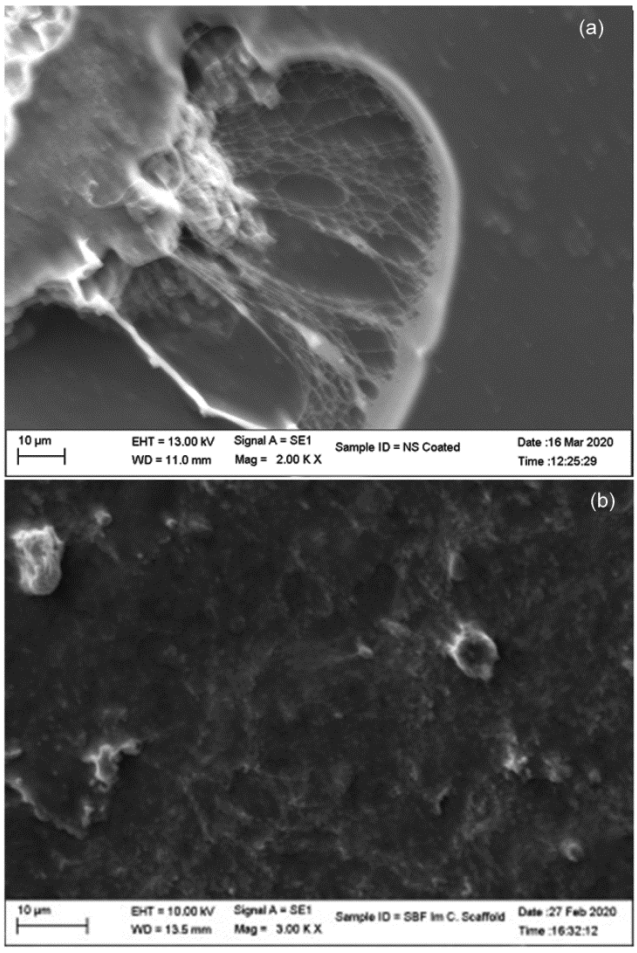

Fig. 8 — SEM micrograph of Ag coated nanofiber (a) Before immersion and (b) After immersion in SBF solution.

calcium phospate mineral regeneration which indicates the bone inductivity. Therefore, these hybrid nanocomposite scaffolds can be suggested as suitable candidate for bone TE. Rather the SEM image of Ag coated PVA/SA scaffold prior to immersion in SBF solution displayed sever damage to scaffold structure due to the coating of Ag NPs. Additionally, it is also evident from the SEM image that the Ag NPs tend to agglomerate severely which clogs the pores of the scaffold.The SEM micrographs of coated scaffold after immersion in the SBF solution displayed the thin layer growth of ECM. However, the formation of the condense matter was found to be superior in PVA/SA/Ag infused nanofibers in comparison with PVA/SA/Ag coated nanofibers. The possible reasons for poor performance of PVA/SA/Ag coated nanofibers was due to blockage of pores by spay coating process which decreased the surface area and hence the bioactivity. Additionally, in PVA/SA/Ag infused scaffolds, the charge interaction of Ag NPs during electrospinning assisted in the formation of nanofibers of smaller diameter (220 nm) with smaller pore size (0.5 µm) compared to PVA/SA fibers with a larger diameter of 250 nm and bigger pore size 0.7 µm. Henceforth, the traditional method of coating nanoparticles on the polymer fibrous matrix was found to ineffective while the newly proposed method of infusing nanoparticle in the polymer solution prior to electrospinning was found to be successful method for scaffold preparation. However, efforts need to be taken in optimizing the electrospinning parameters to obtain continuous fibers with no needle blockage.

Conclusion

This article successfully demonstrates the effectiveness of proposed infusion method for scaffold preparation in comparison with traditional coating

methodology. A suitable supportive scaffold structure that has appropriate topography and biomechanical properties to facilitate bone regeneration (acute haematogenous osteomyelitis) has been obtained. The timely examination of *in vitro* studies of the prepared hybrid scaffolds in the SBF solution signified that these nanofibers have been suitable for TE applications with particular concern for bone regeneration. Thus, we anticipate that the presented paper will contribute to the development of TE and will be a valuable tool for understanding tissue level biology.

Conflict of interest

The authors declare that there is no conflict of interests regarding the publication of this paper.

Acknowledgement

The authors are thankful to the Department of Science and Technology (DST), Science of Equity Empowerment and Development (SEED), CIPET:IPT, Chennai and Biomaterial Development Lab, CIPET:SARP-ARSTPS, Chennai, for providing the necessary supports to carry out above research work.

References

1 Panteli M & Giannoudis P V, *EFORT Open Rev*, 1 (2016) 128.
2 Sheikh Z, Hamdan N, Ikeda Y, Grynpas M, Ganss B & Glogauer M, *Biomater Res*, 21 (2017) 9.
3 Koons G L, Diba M & Mikos A G, *Nat Rev Mater*, 5 (2020) 584.
4 Murugan E & Rangasamy R, *J Biomed Nanotechnol*, 7 (2011) 225.
5 Ao C, Niu Y, Zhang X, He X, Zhang W & Lu C, *Int J BiolMacromol*, 97 (2017) 568.
6 Murugan E, Govindaraju S & Santhoshkumar S, *Electrochim Acta*, 392 (2021) 138973.
7 Murugan E & Gopinath P, *J Mol Catal A Chem*, 294 (2008) 68.
8 Keshvardoostchokami Mina, Majidi S, Huo P, Ramachandran R, Chen M & Liu B, *Nanomaterials*, 11 (2021) 21.
9 Kumar A & Han S S, *Int J Polym Mater Polym Biomater*, 66 (2017) 159.
10 Murugan E & Shanmugam P, *J Nanosci Nanotechnol*, 16 (2016) 426.
11 Jiang X, Xiang N, Zhang H, Sun Y, Lin Z & Hou L, *Carbohydr Polym*, 186 (2018) 377.
12 Yogaraj V, Gowtham G, Akshata C R, Manikandan R, Murugan E & Arumugam M, *J Drug Deliv Sci Technol*, 58 (2020) 101785.
13 Wang J, Lilin Z, Xianhua Z, Runfa W, Lan L & Junchao W, *Front Pharmacol*, 11 (2020) 1.
14 Murugan E, Nimita J, Ariraman M, Rajendran S, Kathirvel J, Akshata C R & Kumar K, *ACS Omega*, 3 (2018) 13685.
15 Mokhena T C & Luyt A S, *Carbohydr Polym*, 165 (2017) 304.
16 Murugan E, Akshata C R, Yogaraj V, Sudhandiran G & Babu D, *Ceram Int*, 48 (2022) 16000.
17 Murugan E, Rani D P G & Yogaraj V, *Colloids Surf B Biointerfaces*, 114 (2014) 121.
18 Kalaivani R, Maruthupandy M, Muneeswaran T, Hemadha B A, Anand M, Ramkritinan C M & Kumaraguru AK, F Lab Medicine, 2 (2018) 22.
19 Sassaki G L, Alexandre H & Rocha O, *Mar Drugs*, 13 (2015) 141.
20 Murugan E, Rani D P G, Srinivasan K & Muthumary J, *Expert Opin Drug Deliv*, 10 (2013) 1319.
21 Ren X, Chen C, Yi H, Min H, Yubao L, Danqing W & Li Z, *Int J Polym Mater Polym Biomater*, 67 (2018) 703.
22 Kalaivani R, Maruthupandy M, Muneeswaran T, Hameedha A, Anand M, Ramakritinan C M & Kumaraguru A K, *Front Lab Med*, 2 (2018) 30.
23 Shameli K, Ahmad M B, Zamanian A, Sangpour P, Shabanzadeh P, Abdollahi Y, Zargar M, *Int J Nanomedicine*, 7 (2012) 5603.
24 Murugan E & Shanmugam P, *Bull Mater Sci*, 38 (2015) 629.
25 Akmaz S, Dilaver E, Yasar M & Erguven O, *Adv Mater Sci Eng*, (2013) 12.
26 Siva A & Murugan E, *Synthesis*, 17 (2005) 2927.
27 El-Hefian E A, Nasef M M & Yahaya A H, *E J Chem*, 7 (2010) 5349.
28 Kane S N, Mishra A & Dutta A K, *Phys Conf Ser*, 755 (2016) 1.
29 Murugan E, Priya A R J, Raman K J, Kalpana K, Akshata C R, Kumar S S & Govindaraju S, *J Nanosci Nanotechnol*, 19 (2019) 7596.
30 Ravi Prakash S D, Ramakrishna H V, Rai S K & Varada A, *J Appl Polym Sci*, 90 (2003) 33.
31 Tadashi Kokubo & Hiroaki Takadama, *Biomaterials*, 27 (2006) 2907.